Role of La_2O_3 in Pd-supported catalysts for methanol decomposition

Cheng Yang, Jie Ren and Yuhan Sun *

State Key Laboratory of Coal Conversion, Institute of Coal Chemistry, Chinese Academy of Science, P.O. Box 165, Taiyuan 030001, People's Republic of China

Received 24 May 2002; accepted 19 August 2002

Systems of Pd supported on various La_2O_3-modified γ-Al_2O_3 and CeO_2–Al_2O_3 catalysts were tested for catalytic methanol decomposition and characterized by means of XRD, BET, TPR, H_2-chemisorption and CO–FTIR. The addition of lanthanum significantly improved the selectivity of CO and H_2 for all the catalysts but showed a different influence on the catalytic activity in two systems. Methanol conversion decreased on La_2O_3-modified Pd/γ-Al_2O_3 catalysts, in line with the reduction of Pd dispersion, while the addition of La_2O_3 improved the dispersion of Pd and reinforced Pd–CeO_2 interaction for La_2O_3-modified Pd/CeO_2–Al_2O_3 catalysts, which resulted in a high production rate of CO and H_2. Thus, a synergistic effect between CeO_2 and La_2O_3 was observed on γ-Al_2O_3-supported Pd catalyst for methanol decomposition.

KEY WORDS: methanol decomposition; La_2O_3; CeO_2; Pd/γ-Al_2O_3; synergistic effect.

1. Introduction

The decomposition of methanol into carbon monoxide and hydrogen is a highly endothermic reaction which has attracted growing interest for its application to energy recovery from waste heat in methanol-fueled automobiles and various industries [1,2]. For such purposes, new catalysts for methanol decomposition must be active at low temperatures (200–250 °C) [2]. Palladium shows an inherent high performance in its reaction with CO, H_2 and methanol [3]. Catalysts containing both lanthanum and palladium were found to be very active in the synthesis of methanol [4–9], but the addition of lanthanum to Pd/γ-Al_2O_3 catalysts tested for the reverse reaction showed low activity, though high selectivity of CO and H_2 was achieved [10]. As a major by-product of Pd/γ-Al_2O_3 for methanol decomposition, dimethyl ether (DME) was produced on the acidic sites [11]. The addition of basic metal modifiers not only neutralizes the surface acidity of γ-Al_2O_3, but Gotti and Prins [8] reported that basic metal oxide additives in contact with the palladium particles also influence its catalytic activity. More recently, Matsumura *et al.* [12–14] studied the effect of cerium on the activity of palladium for methanol decomposition. The authors claimed that high dispersion of palladium particles and the strong interaction between palladium and cerium played important roles in improving the catalyst's activity for low-temperature methanol decomposition. Lanthanum and cerium are termed as same family elements and are quite similar electronically [15]. As is well known with cerium and lanthanum in the petroleum-cracking processes and in TWC systems, the two modifiers together may cause a synergistic promotion in γ-Al_2O_3-supported Pd catalysts for methanol decomposition.

The objective of the present work is to test the methanol conversion as a function of La_2O_3 loading in modified Pd/γ-Al_2O_3 and Pd/CeO_2–Al_2O_3 systems. Differences in the two systems are discussed in relation to the physicochemical properties of the catalysts, which are clarified by the combined use of XRD, BET, TPR, H_2-chemisorption and FTIR techniques.

2. Experimental

2.1. Catalyst preparation

Two series of supports were made by the impregnation of γ-Al_2O_3 ($S_{BET} = 160\,m^2\,g$, Taiyuan, China) with cerium and lanthanum nitrate solutions. The first contained only lanthanum at a nominal La_2O_3 loading varied from 0 to 20 wt%. The second contained both lanthanum and cerium at a nominal CeO_2 loading of 22 wt% and La_2O_3 varied from 0 to 20 wt%, in which the impregnations were performed separately, lanthanum first and cerium second. After the impregnations, all samples were dried and calcined at 500 °C for 4 h. The supported Pd catalysts with Pd loading of 3 wt% were prepared by the wet impregnation method using $PdCl_2$ as the metal precursor compound. The catalysts thus prepared were also dried and calcined at 500 °C for 4 h.

* To whom correspondence should be addressed.
E-mail: yhsun@sxicc.ac.cn

1011-372X/02/1100-0123/0

2.2. Catalytic test

The methanol decomposition reaction was conducted in a flow system under the ambient pressure at 250 °C. The catalyst (1 cm^3) in the micro-reactor was reduced *in situ* with pure hydrogen at 400 °C for 1 h. Methanol (MHSV = 1.8 h^{-1}) was fed into an evaporator by a piston-type pump, then released into the reactor. The analysis was carried out on-stream with gas chromatographs in which an activated carbon column and a Porapak T column were employed.

2.3. Characterization

2.3.1. X-ray powder diffraction and nitrogen physisorption

XRD was carried out with a D/Max-γÅ powder X-ray diffractometer using Ni-filtered Cu K_α radiation. Patterns were recorded from 20 to 70° (2θ) at 40 kV and 40 mA. The surface area of the catalysts was measured at −196 °C by nitrogen adsorption using a BET apparatus (ASAP 2000) after the evacuation at liquid nitrogen temperature and 1 Pa for 3 h.

2.3.2. Temperature-programmed reduction

TPR was carried out using a flow system equipped with a TCD. The mixture of 5 mol% H_2 diluted by argon was used as the reductive gas. The samples of 120 mg in a U-tube quartz reactor were initially flushed with argon of 40 ml/min at 120 °C to remove water, then in the H_2/Ar with a temperature rate of 10 °C/min.

2.3.3. Hydrogen chemisorption

H_2-chemisorption was performed in the TPR equipment. After reduction at 400 °C, the sample of 200 mg was outgassed in argon flow at the same temperature for 30 min and then cooled to 70 °C. Pure hydrogen was passed over the samples at this temperature for 20 min. Under these conditions, β-PdH_x was avoided [16]. The amount of irreversibly adsorbed hydrogen was measured by GC-TCD (Pd/H = 1) and was calibrated by the reduction of pure Ag_2O.

2.3.4. Infrared spectroscopy

FTIR spectra of adsorbed CO were taken in Nicolet Magna 550 spectrometer with a DRIFTS collector accessory. The catalyst (<300 mesh) was put into the sample cup and leveled off. After sealing, pure hydrogen was admitted and the temperature was increased to 400 °C and maintained at that temperature for 2 h. Then, the cell was flushed with argon, cooled down to the ambient temperature, and the background was recorded. CO gas was conducted into a diffuse chamber following purging with argon for 30 min before the IR spectra were recorded.

3. Results

3.1. Catalytic test

Methanol conversion and CO selectivity of La_2O_3-modified Pd/Al_2O_3 and Pd/CeO_2–Al_2O_3 catalysts are shown in figure 1. Methanol conversion on the Pd/Al_2O_3 catalyst was 82.0% with the selectivity of CO only 60.0%. Pd/CeO_2–Al_2O_3 showed higher activity for methanol decomposition than Pd/Al_2O_3. Methanol conversion reached 95.3% and the selectivity of CO was 88.2%. Though DME was produced as the major by-product on Pd/Al_2O_3 and Pd/CeO_2–Al_2O_3 catalysts, the proportion of H_2 and CO production rate was about 2.0 for all the catalysts. The addition of La_2O_3 improved the selectivity of CO remarkably, which was almost 100% even at an La_2O_3 content of only 5 wt%. On La_2O_3-modified Pd/Al_2O_3 catalysts, methanol conversion decreased along with La_2O_3 load increasing from 0 to 20 wt%. But the difference was observed on

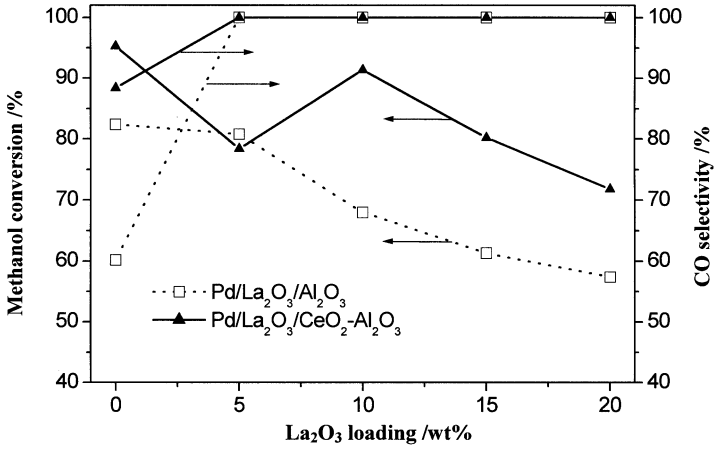

CeO_2 loading=22%, Reaction temperature=250℃, MHSV=1.8 h^{-1}.

Figure 1. Methanol conversion and CO selectivity on various La_2O_3-modified Pd/Al_2O_3 and Pd/CeO_2–Al_2O_3 catalysts.

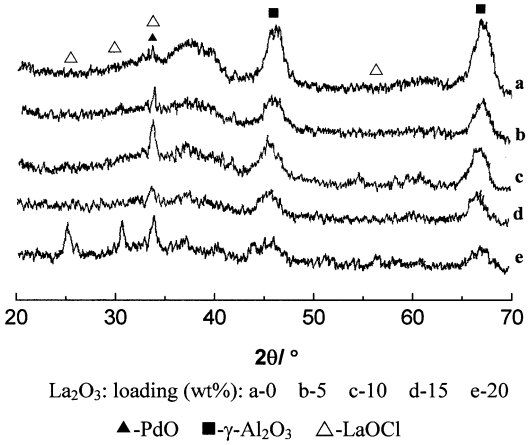

Figure 2. XRD patterns of La_2O_3-modified Pd/Al_2O_3 catalysts.

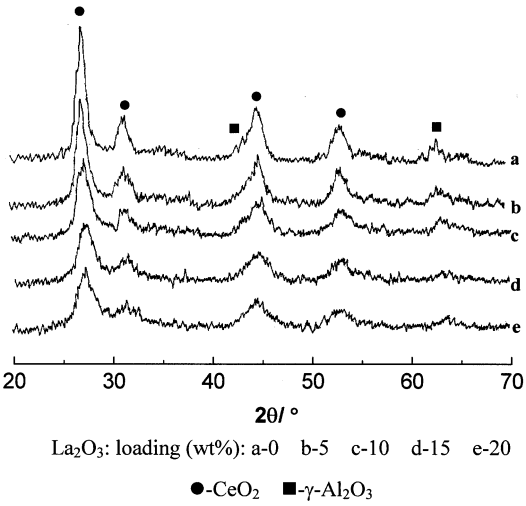

Figure 3. XRD patterns of La_2O_3 modified $Pd/CeO_2–Al_2O_3$ catalysts.

La_2O_3-modified $Pd/CeO_2–Al_2O_3$ catalysts. Methanol conversion decreased somewhat at low content of La_2O_3, then increased with the rise of La_2O_3 content. The activity showed an extreme value at 10 wt% La_2O_3, and then it decreased with La_2O_3 load above 10 wt%. This illustrated that La_2O_3 and CeO_2 in the Pd/γ-Al_2O_3 catalyst performed a synergistic promotion for methanol decomposition.

3.2. XRD

The XRD patterns of Pd/Al_2O_3 and La_2O_3-modified Pd/Al_2O_3 catalysts presented the broad lines due to γ-Al_2O_3 and PdO (see figure 1). The PdO peaks became narrower with the rise of La_2O_3 content, suggesting that the addition of La_2O_3 reduced the dispersion of Pd on γ-Al_2O_3. Some new peaks related to the lanthanum phase appeared when the La_2O_3 content increased up to 20 wt%, though such a content was still below the monolayer coverage on γ-Al_2O_3 [17]. These reflections were due to the formation of LaOCl phases as lanthanum trapped the radial Cl from the Pd precursor during the preparation procedure. Thus, these lanthanum phases might be in close contact with PdO and hinder the palladium dispersion.

Figure 2 shows the XRD patterns of $Pd/CeO_2–Al_2O_3$ and La_2O_3-modified $Pd/CeO_2–Al_2O_3$ catalysts. No reflections of lanthanum species were detected, but well-crystallized CeO_2 was evident. This was in agreement with previous studies that the dispersion of La_2O_3 on γ-Al_2O_3 is significantly higher than CeO_2 upon impregnation from aqueous nitrate solutions [18]. Furthermore, these lines appeared broader for La_2O_3-modified $Pd/CeO_2–Al_2O_3$, suggesting that it contained somewhat smaller CeO_2 crystals compared to $Pd/CeO_2–Al_2O_3$. As Zintl and Croatto [19] reported, La^{3+} ions could be dissolved into the CeO_2 lattice due to a similarity of ionic radii ($La^{3+} = 0.119$ nm, $Ce^{4+} = 0.109$ nm). So an $La_2O_3–CeO_2$ solid solution could be formed, which improved the dispersion of CeO_2 and prevented the formation of LaOCl species. Apparently, the reflection peaks corresponding to CeO_2 became slightly broader with the increase of La_2O_3 content, possibly due to the formation of more $La_2O_3–CeO_2$ solid solution. No reflections of PdO appeared in $Pd/CeO_2–Al_2O_3$ or La_2O_3-modified $Pd/CeO_2–Al_2O_3$, indicative of a high dispersion of Pd in these samples.

3.3. Surface area and H_2-chemisorption

The surface areas of all catalysts are given in table 1. Pd/Al_2O_3 showed the highest BET surface area of all the catalysts. This was slightly reduced by the addition

Table 1
BET surface areas and Pd dispersion of various La_2O_3-modified Pd catalysts.

La_2O_3 loading (wt%)	S_{BET} (m^2/g)		Pd dispersion (%)[a]	
	$Pd/La_2O_3/Al_2O_3$	$Pd/La_2O_3/CeO_2–Al_2O_3$	$Pd/La_2O_3/Al_2O_3$	$Pd/La_2O_3/CeO_2–Al_2O_3$
0	151.4	118.3	31.1	37.7
5	144.1	130.3	28.3	39.0
10	138.7	122.0	21.7	46.1
15	136.1	120.9	17.1	45.3
20	132.9	120.6	13.2	43.9

[a] Calculated by the results of hydrogen chemisorption.

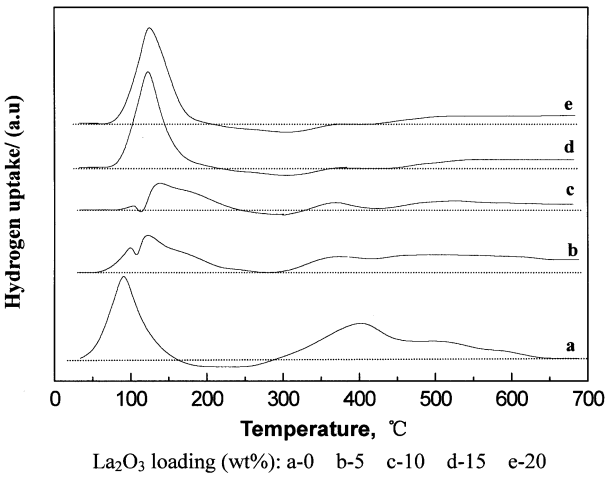

La_2O_3 loading (wt%): a-0 b-5 c-10 d-15 e-20

Figure 4. TPR profiles of La_2O_3-modified Pd/Al_2O_3 catalysts.

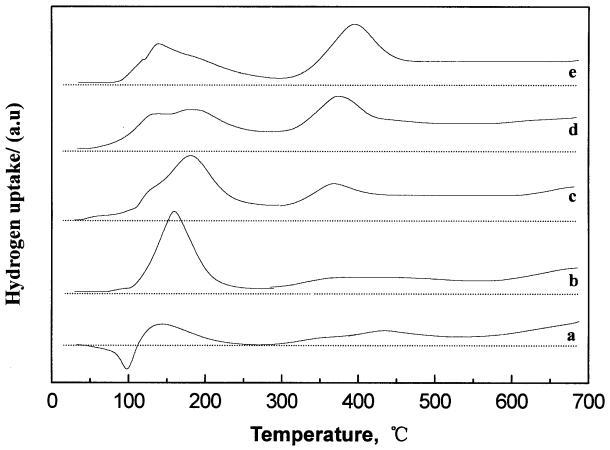

La_2O_3 loading (wt%): a-0 b-5 c-10 d-15 e-20

Figure 5. TPR profiles of La_2O_3-modified Pd/CeO_2–Al_2O_3 catalysts.

of La_2O_3. Though some LaOCl was formed as observed by XRD, the textural structure of γ-Al_2O_3 was not changed. The surface area of Pd/CeO_2–Al_2O_3 was low due to large CeO_2 particles aggregated on the orifices of the γ-Al_2O_3 support [20]. It was interesting to find that a relatively high surface area was achieved in La_2O_3-modified Pd/CeO_2–Al_2O_3. The phenomenon was interpreted as highly dispersed La_2O_3 and CeO_2 that had spread well over the surface of γ-Al_2O_3 combined with XRD results. The areas of La_2O_3-modified Pd/CeO_2–Al_2O_3 were also slightly reduced along with the increase of La_2O_3 content.

The Pd dispersion of Pd/Al_2O_3 was not high according to the hydrogen chemisorption data in table 1. As observed by XRD, the addition of La_2O_3 reduced the Pd-dispersed degree in the $Pd/La_2O_3/Al_2O_3$ catalyst. It can be seen that the Pd dispersion of Pd/CeO_2–Al_2O_3 was high. This agrees with the XRD results and that of Alexandrouh and Nix observed by XPS [21]. Contrary to the results of the modified Pd/Al_2O_3 system, the addition of La_2O_3 improved the Pd dispersion in the modified Pd/CeO_2–Al_2O_3 system. It was observed that relatively high loading of La_2O_3 at about 10 wt% had an effective promotion.

3.4. TPR

The reduction behaviors of Pd/Al_2O_3 and La_2O_3-modified Pd/Al_2O_3 catalysts are illustrated in figure 4. The reduction of PdO in Pd/Al_2O_3 occurred at the temperature range 50–180 °C with a maximum peak at 80 °C. The other peak of H_2 consumption appeared above 300 °C, corresponding to the removal of surface oxygen on γ-Al_2O_3. The addition of La_2O_3 not only masked off the H_2 consumption peaks of γ-Al_2O_3, but also hindered the reduction of PdO as evidenced by the shift of the peaks to high temperatures. The phenomena became distinctive with La_2O_3 load increase. The maximum reduction rate occurred at about the same temperature (peaks at 90 °C and 120 °C) for La_2O_3-modified Pd/Al_2O_3 with an La_2O_3 load of 5 and 10 wt%, with only one peak at about 110 °C for that of 15 and 20 wt%. As mentioned above, LaOCl phases were formed and, therefore, an interaction between Pd and its vicinal LaOCl phases existed. It seemed that all Pd particles on γ-Al_2O_3 were in close contact with LaOCl when the La_2O_3 load was more than 10 wt%.

CeO_2 enhanced the reduction rate of PdO greatly, which occurred at room temperatures (see figure 5(a)). Afterwards, a negative peak appeared due to hydrogen desorption from metallic Pd. The oxygen species of CeO_2 were easily removed by hydrogen molecules activated by Pd, and then a synergistic reduction between Pd and CeO_2 occurred as described by Yao and Yao [22]. Thus, the hydrogen consumption in the range of 100–250 °C was assigned to the reduction of surface oxygen capping CeO_2. The peak visible in the TPR profile with a maximum near 440 °C could be associated with the reduction of oxygen anions in the interface of CeO_2 and γ-Al_2O_3; the other beginning at about 600 °C was the reduction of bulk CeO_2 shifted downward due to Pd promotion [22]. For La_2O_3-modified Pd/CeO_2–Al_2O_3 catalysts (see figure 5(b–e)), a new peak was observed near 350 °C due to the partial reduction of La_2O_3 in the vicinity of Pd [23]. Similar to that of the La_2O_3-modified Pd/Al_2O_3 system, the addition of La_2O_3 hindered the reduction of PdO in the Pd/CeO_2–Al_2O_3 system. The PdO reduction peaks toward higher temperatures overlapped with the reduction peak of surface oxygen capping CeO_2. On the other hand, La_2O_3 enhanced the removal of lattice oxygen in bulk CeO_2. Following the reduction of oxygen anions in the interface of CeO_2 and γ-Al_2O_3, hydrogen was consumed at a constant rate by elevating the temperature. As a matter of fact, the dissolution of La^{3+} ions into the CeO_2 lattice resulted in the formation of more oxygen vacancies because of charge neutralization. This enhanced the availability of lattice oxygen of the bulk CeO_2, as Graham [24] observed. The lattice oxygen of

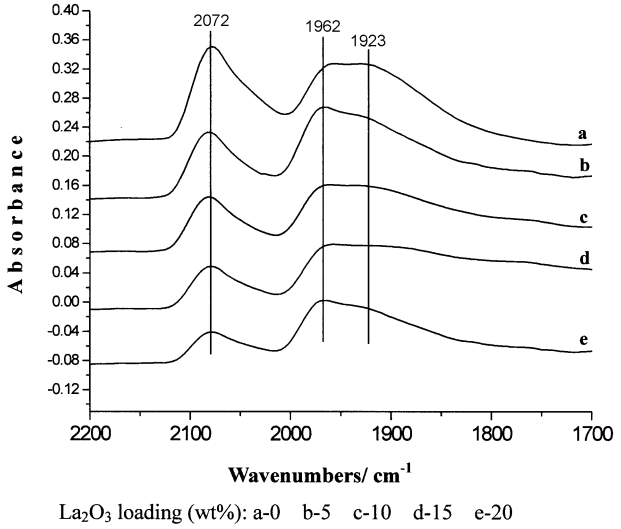

Figure 6. FTIR spectra of CO adsorbed on La_2O_3-modified Pd/Al_2O_3 catalysts.

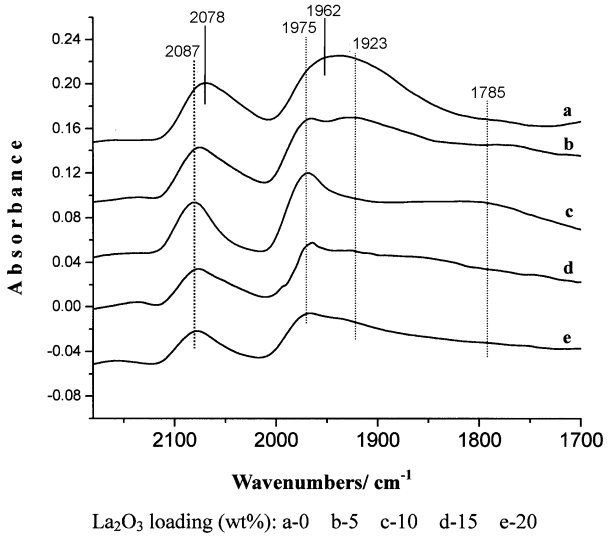

Figure 7. FTIR spectra of CO adsorbed on La_2O_3-modified Pd/CeO_2–Al_2O_3 catalysts.

CeO_2 diffused into the Pd–CeO_2 interface and reacted with hydrogen activated by Pd (probably spilled over hydrogen) at a constant rate with the temperature elevated.

3.5. CO–FTIR

The IR spectra of CO adsorbed on Pd/Al_2O_3 illustrated that (see figure 6) the sharp bands present at 2072 cm^{-1} were assigned to CO bonded on Pd^0 surface sites in linear forms, while those at 1962 and 1923 cm^{-1} were attributed to the bridged forms on Pd(100) and Pd(111) surfaces, respectively [25]. In comparison with Pd/Al_2O_3, the spectra of La_2O_3-modified Pd/Al_2O_3 catalysts showed less intense bands of linear CO and more bridged forms, while the CO stretching frequencies either for linearly or bridged forms were almost the same. This implied that the addition of La_2O_3 did not change the electronic state of Pd. The intense bands decreased with the increase of La_2O_3 content, perhaps due to the decrease of Pd dispersion.

With the presence of CeO_2, the intensity of CO both linearly and bridged bonded on Pd was suppressed due to the Pd–CeO_2 interaction (see figure 7(a)) [26]. Noteworthy was that the bands on La_2O_3-modified Pd/CeO_2–Al_2O_3 catalysts at 2078 cm^{-1} progressively shifted to 2087 cm^{-1}, while those at 1962 cm^{-1} shifted to 1975 cm^{-1} (see figure 7(b–e)). These illustrated that the bands underwent a blue shift due to the charge transfer from Pd to the support. As a result, the palladium had a lower electron density than Pd^0, *i.e.*, electron-deficient $Pd^{\sigma+}$ species existed due to the reinforcement of the interaction between Pd and CeO_2 by La_2O_3. The intensity of these bands decreased to some degree with the increase of La_2O_3 content. Furthermore, a wide band appearing at about 1785 cm^{-1} could be assigned to the adsorption of CO at the metal/support interface (*i.e.*, C bonded to Pd and O to Ce^{3+}) [27], being characteristic of the interaction between the metal and the reducible CeO_2. It has been reported that the Pd–CeO_2 interface played an important role in the improvement of the interaction between Pd and CeO_2, which might be responsible for the charge transfer [13].

4. Discussion

Lanthanum has become well known as a promoter in many catalytic systems. Pd- and La_2O_3-containing catalysts, with or without SiO_2 support have been widely studied for methanol synthesis from CO and H_2. For the reverse reaction, Pd/γ-Al_2O_3 appeared to be active at low temperatures with a considerable amount of DME as a major by-product [28]. DME is produced by methanol dehydration, which is an exothermic reaction, due to the surface acidity. The addition of La_2O_3 neutralized the surface acidic sites on γ-Al_2O_3 [10]. Thus, the selectivity of CO and H_2 reached about 100%, but the activity decreased remarkably. CeO_2 was found to significantly promote the function of Pd for catalytic methanol decomposition [13]. In the previous work, CeO_2 was used as a modifier to the Pd/Al_2O_3 system for this reaction and a high load of CeO_2 of about 22 wt% showed effective promotion for the catalytic activity, but still with some DME produced [29]. This was due to CeO_2 partly suppressing the acidic sites on γ-Al_2O_3 or new kinds of acidic sites generated, which were discussed in ref. [28].

For the purpose of high activity for methanol decomposition meanwhile, with high selectivity to CO and H_2, La_2O_3 was further introduced to the Pd/CeO_2–Al_2O_3 system. But a different action of methanol conversion as a function of La_2O_3 load was observed. From our point of view, the activity of the catalysts was determined

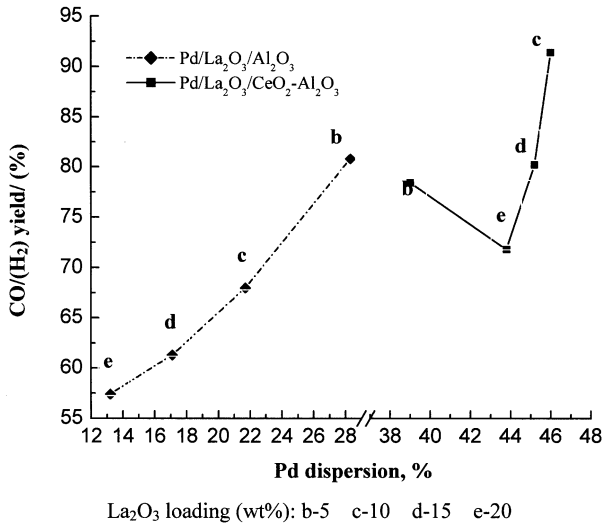

Figure 8. The relationship between Pd dispersion and the production rate of CO/(H_2) on La_2O_3-modified Pd/Al_2O_3 and Pd/CeO_2–Al_2O_3 catalysts.

by both the dispersion and the electronic state of Pd. The modifiers were in contact with the palladium particles, but the role of lanthanum in the two systems was not the same.

For the La_2O_3-modified Pd/Al_2O_3 system, a direct relationship between Pd dispersion and the yield of H_2 and CO was observed (see figure 8). Usually a model of SMSI was proposed to explain the role of lanthanum in the promotion of the Pd catalytic activity. In this case, Pd particles were decorated by "LaOx patches", then a transfer of the excess charge of La to Pd in the Pd–LaOx interface was found by XPS, giving rise to the Pd state as an electron-donor over Pd^0 [5]. In our experimental results, an interaction between Pd and lanthanum also occurred, which decreased the dispersion of Pd and hindered the reduction. However, the lanthanum phase was LaOCl in the catalysts as detected by XRD. The oxygen corresponding to this phase could not be removed during the TPR process, and no "LaOx patches" formed. The palladium was confirmed to be in the Pd^0 state by FTIR. Thus, the role of lanthanum mainly influenced the dispersion of Pd, which resulted in the decrease of the catalytic activity for methanol decomposition into CO and H_2.

High Pd dispersion was achieved in the La_2O_3-modified Pd/CeO_2–Al_2O_3 system, which showed a relatively high activity for methanol decomposition. However, the yield of CO and H_2 was not directly related to the dispersion of Pd, as illustrated in figure 8. Ponec [30] pointed out that Pd^+ species are active in methanol synthesis. In the case of methanol decomposition, the cationic palladium species was also considered to be highly active, and such species could be produced by the interaction between Pd particles and support. However, the intimate contact between Pd particles and CeO_2 on γ-Al_2O_3 was reported to be restricted by a $CeAlO_3$ compound formation [31]. To avoid such an effect, La_2O_3 as a γ-Al_2O_3 modifier was introduced to block the reaction of γ-Al_2O_3 and CeO_2. In agreement with these studies, a stronger interaction between Pd and CeO_2 took place in the present La_2O_3-modified Pd/CeO_2–Al_2O_3 system. As a result, palladium was in an electron-deficient state ($Pd^{\sigma+}$). Meanwhile, a high dispersion of palladium and CeO_2 particles was achieved on the γ-Al_2O_3 support. The lanthanum phase was maintained as La_2O_3 and could be reduced into "LaOx patches". Shen and Matsumura [13] proposed that a kind of chemical bond, such as Pd–O–Ce, was formed in the Pd–CeO_2 interface due to their strong interaction, which accounted for the formation of cationic palladium species like that of Pd–O–Zr. The production rate of CO and H_2 was determined by the quantity of catalytic sites ($Pd^{\sigma+}$). In the La_2O_3-modified Pd/CeO_2–Al_2O_3 system, more Pd–O–Ce bonds were formed with the increase of La_2O_3 content and reached a maximum with the content of La_2O_3 at about 10 wt%. However, at higher loading of La_2O_3, the interaction between Pd and CeO_2 by Pd–O–Ce bonds could be interrupted probably as "LaOx Patches" formed at the Pd–CeO_2 interface. Thus, the synergistic effect of CeO_2 and La_2O_3 in γ-Al_2O_3-supported Pd catalysts for methanol decomposition into CO and H_2 was clearly understood.

5. Conclusions

Lanthanum effectively improved the selectivity of Pd-supported catalysts for methanol decomposition into CO and H_2. In the lanthanum-modified Pd/Al_2O_3 system, the catalytic activity decreased along with the rise of La_2O_3 content, in line with the results that Pd dispersion decreased due to the Pd–LaOCl interaction. The production rate of CO and H_2 on the Pd/CeO_2–Al_2O_3 catalyst was significantly improved by the addition of a certain amount of La_2O_3 (10 wt%). This contributed to the increase of Pd dispersion as well as the reinforcement of the Pd–CeO_2 interaction.

A model for the strong interaction between Pd and CeO_2 by a Pd–O–Ce bond at the interface of highly dispersed Pd and CeO_2 particles was proposed. In this case, lanthanum was found to reinforce or interrupt the Pd-interaction, depending on the La_2O_3 loading. Thus, CeO_2 and La_2O_3 performed a synergistic effect on γ-Al_2O_3-supported Pd catalyst for methanol decomposition into CO and H_2.

Acknowledgment

The authors gratefully acknowledge the funding of this project by the Natural Science Foundation of China (Project ID 991010).

References

[1] H. Yooh, M.R. Stouffer, P.J. Duolt, F.P. Burke and G.P. Curran, Energy Prog. 5 (1985) 78.
[2] Y. Matsumra, N. Tode, T. Yazawa and M. Haruta, J. Mol. Catal. A: Chem. 99 (1995) 183.
[3] S.I. Mamura, K. Denpo, K. Utani, Y. Matsumura and H. Kanai, React. Kinet. Catal. Lett. 67 (1999) 163.
[4] M. Rebholz and N. Kruse, J. Chem. Phys. 95 (1991) 7745.
[5] T.H. Fleisch, R.F. Hicks and A.T. Bell, J. Catal. 87 (1984) 398.
[6] R.F. Hicks and A.T. Bell, J. Catal. 90 (1984) 205.
[7] J.M. Driessen, E.K. Poels, J.P. Hindermann and V. Ponec, J. Catal. 82 (1983) 26.
[8] A. Gotti and R. Prins, J. Catal. 175 (1998) 302.
[9] G. Mul and A.S. Hirschon, Catal. Today 65 (2001) 69.
[10] D.T. Wickham, W. Logsdon, S.W. Cowley and C.D. Butler, J. Catal. 128 (1991) 198.
[11] S.H. Ali and J.G. Goodwin, Jr, J. Catal. 171 (1997) 333.
[12] Y. Usami, K. Kagawa, Y. Matsumura, H. Sakurai and M. Haruta, Appl. Catal. 171 (1998) 123.
[13] W.J. Shen and Y. Matsumura, Phys. Chem. Chem. Phys. 2 (2000) 1519.
[14] W.J. Shen and Y. Matsumura, J. Mol. Catal. A: Chem. 153 (2000) 165.
[15] A.B. Stiles, *Catalyst Supports and Supported Catalysts* (Elsevier, Butterworths, 1987).
[16] P.C. Aben, J. Catal. 10 (1968) 224.
[17] M. Ozawa and M. Kimura, J. Mater. Surf. Sci. Lett. 9 (1990) 291.
[18] T. Miki, T. Ogawa, M. Haneda, N. Kaluta, A. Ueno, S. Yateishi, S. Matsura and M. Sato, J. Phys. Chem. 94 (1990) 6464.
[19] E. Zintl and U.Z. Croatto, Anorg. Allg. Chem. 242 (1939) 79.
[20] G. Groppi, C. Cristiani, L. Lietti, C. Ramella, M. Valentini and P. Forzatti, Catal. Today 50 (1999) 399.
[21] M. Alexandrouh and M. Nix, Surf. Sci. 321 (1994) 47.
[22] H.C. Yao and F.Y. Yao, J. Catal. 86 (1984) 254.
[23] J.S. Rieck and A. Bell, J. Catal. 96 (1995) 88.
[24] G.W. Graham, P.J. Schnitz, R.K. Usmen and R.W. Mccbe, Catal. Lett. 17 (1993) 175.
[25] A. Badri, C. Binet and J.C. Lavalley, J. Chim. Phys. Phys.-Chim. Biol. 92 (1995) 133.
[26] R.S. Monteiro, L.C. Dieguez and M. Schmal, 16th NACS, PII-104.
[27] S. Boujana, D. Demri and J. Cressely, Catal. Lett. 7 (1990) 359.
[28] N. Iwasa, O. Yamamoto, T. Akazawa, S. Ohyama and N. Takezawa, J. Chem. Soc. Chem. Commun. 113 (1991) 1322.
[29] C. Yang, J. Ren and Y.H. Sun, J. Rare Earth. 19 (2001) 67.
[30] J.C. Ponec and S.A. Ausen, J. Catal. 58 (1979) 131.
[31] J.Z. Shyu, W.H. Weber and H.S. Gandhi, J. Phys. Chem. 92 (1988) 4964.